



## Original Paper

# Effect of nanocomposite pour point depressant EVAL/CNT on flow properties of waxy crude oil



Yang Liu <sup>a</sup>, Zheng-Nan Sun <sup>a</sup>, Sheng-Zhu Ji <sup>b</sup>, Yi-Hai Yang <sup>a</sup>, Jian-Qi Xu <sup>a</sup>, Guo-Lin Jing <sup>a,\*</sup>

<sup>a</sup> Provincial Key Laboratory of Oil & Gas Chemical Technology, College of Chemistry & Chemical Engineering, Northeast Petroleum University, Daqing, 163318, Heilongjiang, China

<sup>b</sup> No. 8 Oil Production Plant Engineering Technology Brigade, Daqing Oilfield, Daqing, 163514, Heilongjiang, China

## ARTICLE INFO

## Article history:

Received 20 November 2022

Received in revised form

12 February 2023

Accepted 20 May 2023

Available online 22 May 2023

Edited by Jia-Jia Fei

## Keywords:

Pour point depressant

Carbon nanotubes

Nanocomposites

Waxy crude oil

Rheological behavior

## ABSTRACT

The nanocomposite EVAL-CNT was produced by chemical grafting in the solution system through the esterification of ethylene-vinyl alcohol copolymer (EVAL) and carboxylated multi-walled carbon nanotubes (O-MWCNT), and its structural properties were characterized. The improvement of the rheological properties of the waxy oil system by the novel pour point depressant was investigated using macroscopic rheological measurements and microscopic observations. The results showed that EVAL-CNT nanocomposite pour point depressant (PPD) could significantly reduce the pour point and improve the low temperature fluidity of crude oil and had better performance than EVAL-GO at the same addition level. The best effect was achieved at the dosing concentration of 400 ppm, which reduced the pour point by 13 °C and the low-temperature viscosity by 85.4%. The nanocomposites dispersed in the oil phase influenced the precipitation and crystallization of wax molecules through heterogeneous crystallization templates, which led to the increase of wax crystal size and compact structure and changed the wax crystal morphology, which had a better effect on the rheological properties of waxy oil.

© 2023 The Authors. Publishing services by Elsevier B.V. on behalf of KeAi Communications Co. Ltd. This is an open access article under the CC BY-NC-ND license (<http://creativecommons.org/licenses/by-nc-nd/4.0/>).

## 1. Introduction

Paraffins usually represent *n*-alkanes in the carbon number range C<sub>16</sub>–C<sub>40</sub>, which are dissolved in crude oil in equilibrium at relatively high temperatures (Aiyejina et al., 2011; Martinez-Palou et al., 2011). When the temperature is below wax appearance temperature (WAT), the wax molecules start to crystallize and precipitate due to supersaturation. When the concentration of wax crystals accumulates to a degree, the spatial network structure can be formed between the wax crystals to encapsulate the flowable liquid oil, thus the crude oil overall loses its fluidity and forms a gelling structure, and the waxy crude oil becomes a gel system (Chen et al., 2019; Chi et al., 2019; Lei et al., 2016). Wax crystallization will increase the adhesion of crude oil, and cause the viscosity of crude oil to increase, leading to the loss of pipeline pressure and reducing the effective transmission capacity of crude oil pipeline (Moud, 2022; Soni et al., 2010; Subramanie et al., 2021; Xu et al., 2013). After the pipeline is stopped, the crude oil in a non-

Newtonian state will re-gather and precipitate as its temperature decreases, and the interaction will finally form a spatial network structure, and the interaction between wax crystals will then be enhanced, which increases the difficulty of restarting the stopped transmission; in addition, the deposition of wax crystals in the transmission system may also cause many difficulties in the transmission and production and other related fields (Wang et al., 2022).

The chemical modification of waxy crude oils by adding small quantities of polymeric PPD to waxy crude oils has become an effective approach to improve the efficiency of crude oil pipelines. Ethylene vinyl acetate (EVA) copolymer is widely used as PPD for crude oil extraction and crude oil pipeline transportation and is also a successful commercial PPD (Zhang et al., 2022). However, traditional polymeric PPDs still suffer from weak resistance to repeated heating and shearing, and selective effects on waxy crude oils. The development of novel high-efficiency polymeric PPDs and the revelation of their mechanism of action have become crucial technical issues to be discussed in engineering applications (Alves et al., 2023; Oliveira et al., 2016; Yang et al., 2019b).

Polymer/inorganic nanocomposites can retain the original

\* Corresponding author.

E-mail address: [jglxueshu@yeah.net](mailto:jglxueshu@yeah.net) (G.-L. Jing).

properties of polymers while maintaining the excellent mechanical properties, heat resistance and special optical, electrical and magnetic properties of inorganic particles (Colunga et al., 2021; Elmesallamy et al., 2022). In the past few years, there has been extensive interest in studying the performance of nanomaterials and polymers (Huang et al., 2020b; Kashefi et al., 2021), clays and polymers (Al-Sabagh et al., 2016a; Huang et al., 2020a; Subramanie et al., 2021; Wang et al., 2020), or nanohybrids composed of carbon nanostructures and polymers (Al-Sabagh et al., 2016b) as PPDs for waxy crude oil. The role of graphene oxide nanostructures in enhancing the flow of crude oil has become a popular research topic in recent years (Ding et al., 2018; Jaber et al., 2020; Liang et al., 2022; Mahmoud and Betiha, 2021; Qu et al., 2022; Zhao et al., 2018). The oxygen-containing groups on graphene oxide may be involved in the inhibition of wax growth through a surface adsorption mechanism. The adsorption of nanohybrid molecules on the surface of wax molecules deactivates the wax core, thus preventing further growth of the wax. As a result, crystals of wax molecules appear very small in size or highly dispersed in the crude oil, thereby inhibiting the reticulation necessary for solidification.

When mentioning nanostructured carbon materials (as illustrated in Fig. 1), it is impossible to ignore the important role that carbon nanotubes perform in various fields (Lin et al., 2003; Ma et al., 2022; Mu et al., 2022; Wu et al., 2013a, 2018b). Carbon nanotube is a new type of seamless, hollow tubular nanomaterial formed by coiling graphene sheets with carbon atoms  $sp^2$  hybridized (Chen et al., 2001; Lin et al., 2021). The unique electrical, structural, thermal, and mechanical properties of carbon nanotubes can be used to enhance the properties of composite materials (Wu et al., 2013b, 2018a). The main method of covalent modification of MWCNTs is to use strong oxidizing agents such as concentrated  $H_2SO_4$  and concentrated  $HNO_3$  to introduce functional groups such as carboxyl or hydroxyl groups into the ports of MWCNTs and locations where certain defects exist on the tube walls (Datsyuk et al., 2008). It is only in the recent two years that studies of carbon nanotubes in the oil field have started to emerge (Li et al., 2020; Sepehrnia et al., 2022; Singh et al., 2021). Alemi et al. (2021a) investigated the effect of single-walled carbon nanotubes in controlling the formation and size growth of asphaltene particles and wax crystals under practical production conditions. They found that crude oil treated with SWCNTs resulted in changes in both size and structure of wax crystals, which also confirmed the interaction between carbon nanotubes and the active sites of wax crystals. Carbon nanotubes can act as effective inhibitors and dispersants to stabilize the aggregation rate of waxes and asphaltenes under high pressure-high temperature conditions. The nanocomposite MWCNT- $Fe_2O_3$  was prepared by Alemi et al. (2021b) to control asphaltene particle formation and growth in unstable crude oil. The

inhibition and dispersion properties of the synthesized composites on asphaltene precipitation were observed by microscopy.

Inspired by this, as well as combining the previous theoretical and experimental research base, the author came up with the idea of combining carbon nanotube materials and modified conventional PPDs in an experimental approach to preparing novel PPDs. The author compounded traditional PPD with carbon nanotube materials and introduced carbon nanotube composites into the field of crude oil transportation based on the previous work (Liu et al., 2021). Through pour point experiments and rheological analysis, the influence of the novel nanocomposite PPD on the rheological improvement effect of waxy oil has been investigated, and the mechanism of the interaction between carbon nanomaterials and wax crystals has been further revealed through the microscopy of wax crystals. The PPD dosage rate is also an important economic indicator in the engineering field, and the study of dosage-regulated rheology improvement of waxy crude oil is also the key focus of this research.

## 2. Experimental section

### 2.1. Materials

The oil sample used in this paper was obtained from Daqing Oilfield, Heilongjiang, China, which is typical waxy crude oil. The basic physical parameters and measurement standards of crude oil are shown in Table 1. It was carried out in triplicate and the error calculated for this measurement also considered the uncertainties of the thermometer ( $0.3\text{ }^\circ\text{C}$ ) and the analytical balance ( $0.0002\text{ g}$ ). Methanol (AR), toluene (AR), dodecane (AR), sodium hydroxide (NaOH), and N-heptane were all acquired from Aladdin Reagent Co., Ltd. (Shanghai). In addition, the vinyl acetate (VA) of EVA applied here is 26 wt%, which was obtained from Mitsui Chemicals (Japan). Carboxylated multi-walled carbon nanotubes (O-MWCNT) were purchased from Zhongsen Linghang Technology Co., Ltd. (Shenzhen, China). The EVAL used here was synthesized based on the method mentioned in a previous paper (Liu et al., 2021).

### 2.2. Preparation of EVAL-CNT nanocomposite

Using the previously synthesized EVAL product, the chemical

**Table 1**  
Physical characteristics of waxy crude oil.

Parameter	Results	Methods
Wax, wt%	20.16	SY/T 7550-2012
Resin, wt%	8.52	SY/T 7550-2012
Asphaltene, wt%	1.59	SY/T 7550-2012
Pour point, $^\circ\text{C}$	34	ASTM D-97

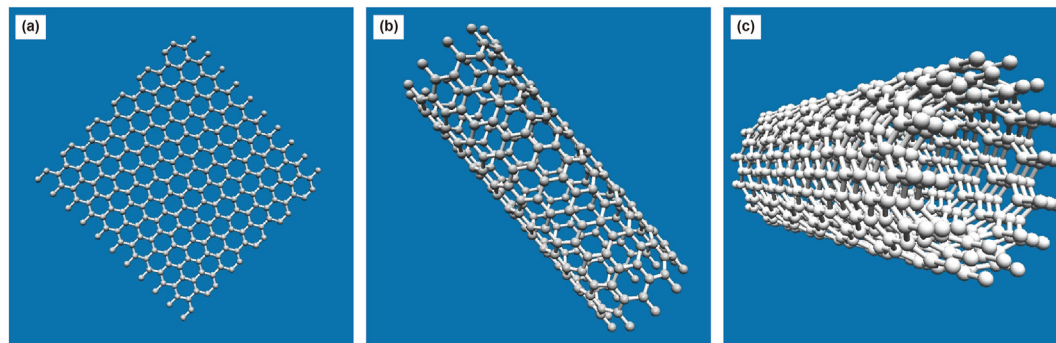


**Fig. 1.** Structural schematic of carbon nanomaterials: (a) graphene; (b) single-walled carbon nanotubes; (c) multi-walled carbon nanotubes.

grafting process was completed by the esterification reaction between the hydroxyl group on EVAL and the carboxylate group on the carboxylated multi-walled carbon nanotubes to form a new nanocomposite named EVAL-CNT, and the synthesis route diagram is shown in Fig. 2. The specific experimental steps are described as follows: carboxylated carbon nanotubes were added to toluene and the suspension was sonicated for 30 min to make it uniformly dispersed, while EVAL was completely dissolved in toluene on the other side, and then the carbon nanotube solution was added to the EVAL solution, and the reaction was thoroughly mixed at 90 °C for 2 h. According to the mass fraction ratios of O-MWCNT to EVAL, two types of nanocomposites were synthesized noted as EVAL-0.5% CNT and EVAL-1% CNT.

### 2.3. Characterization of synthesized additives

The Fourier transition infrared spectrometry (Tensor 27, Bruker, USA) was used to perform FTIR analysis in the wavenumber range of 4000–400  $\text{cm}^{-1}$ . Thermogravimetric analysis (TGA) was performed using an HTG-1 thermogravimetric differential thermal analyzer at a heating rate of 10 °C/min to analyze the weight loss of the synthesized products. The samples were heated from room temperature to 800 °C under a nitrogen atmosphere. The morphology of nanostructure was assessed with the scanning electron microscope (SEM, JSM-6510LV, Zeiss, Germany) operated at 30 kV.

### 2.4. Pour point test

The pour point, an essential indicator of crude oil liquidity performance evaluation, is the minimum temperature at which the oil flows and can be pumped. The pour point of the oil sample before and after adding the nanocomposite PPDs was measured based on the method mentioned in the standard ASTM D97-17a (Mahmoud and Betiha, 2021). Each experiment was repeated three times to verify the pour point and the uncertainty bars were presented in the corresponding figs.

### 2.5. Rheological properties of untreated and treated crude oil

A DHR-1 Advanced Hybrid Rheometer (TA Instruments, USA) was applied to measure the rheological properties of the untreated/treated waxy crude oil. All oil samples were preheated at 60 °C for an hour to eliminate the hot history. Each test was run three times to verify the repeatability, and the maximum error in the distribution of test results was within a reasonable range of  $\pm 2.0\%$ . Thereafter, only the average data was reported.

#### 2.5.1. Viscosity-temperature curve measurement

The preheated oil samples were loaded into the rheometer and held at a constant temperature of 60 °C for 20 min. A constant shear rate (20  $\text{s}^{-1}$ ) was applied to the crude oil and the variation of apparent viscosity with temperature drop was monitored at a cooling rate of 0.5 °C/min from 60 to 15 °C (Yao et al., 2018).

#### 2.5.2. Viscoelastic curve measurement

The viscoelasticity laboratory in oscillatory mode is an effective way to study the sol-gel transition process of oil samples under static cooling conditions (Sharma et al., 2019). The preheated oil samples were put into the rheometer and kept at a constant temperature of 60 °C for 20 min, and then oscillated at a cooling rate of 0.5 °C/min to 15 °C, and the strain of the rheometer was set to 0.0005 and the oscillation frequency was 1 Hz (Yang et al., 2019a). Due to the high precision of the rheometer, the standard error of the gel point measurement was  $\pm 0.2$  °C. For comparative purposes, virgin crude oil and oil doped with EVAL were measured to be used as reference samples.

#### 2.5.3. Rheological performance test

The preheated oil sample was loaded into the rheometer, and the cooling rate was controlled to be 0.5 °C/min from 60 to 15 °C to form a stable gel structure, and then the temperature was kept at 15/25/35 °C for 30 min, followed by the controlled shear rate from 5–200  $\text{s}^{-1}$  within 10 min to measure the rheological curve of the oil sample (Sharma et al., 2022; Xia et al., 2022a).

#### 2.5.4. Yield properties

The oil samples were cooled from 60 to 15 °C at 0.5 °C/min and then placed at a constant temperature of 15 °C for 30 min. The change of the strain value with the shear stress was measured by the continuously increasing shear rate, applying the shear rate from 5–200  $\text{s}^{-1}$  within 10 min to obtain the stress-strain curves (He et al., 2016; Xia et al., 2022b). When there is a sudden linear increase in the strain value, the corresponding stress is defined as the yield stress of the oil sample.

### 2.6. Polarized optical microscopy observation

A polarized optical microscope (ZEISS AXIO, Germany) was used to observe the wax crystal morphology of the oil sample before and after the addition of nanocomposite PPD at a certain temperature. The oil samples were heat-treated at 60 °C for 20 min, then loaded onto the microscope hot stage and cooled down from 60 to 15 °C at a cooling rate of 0.5 °C/min, and polarized micrographs of the oil samples at 15 °C were taken.

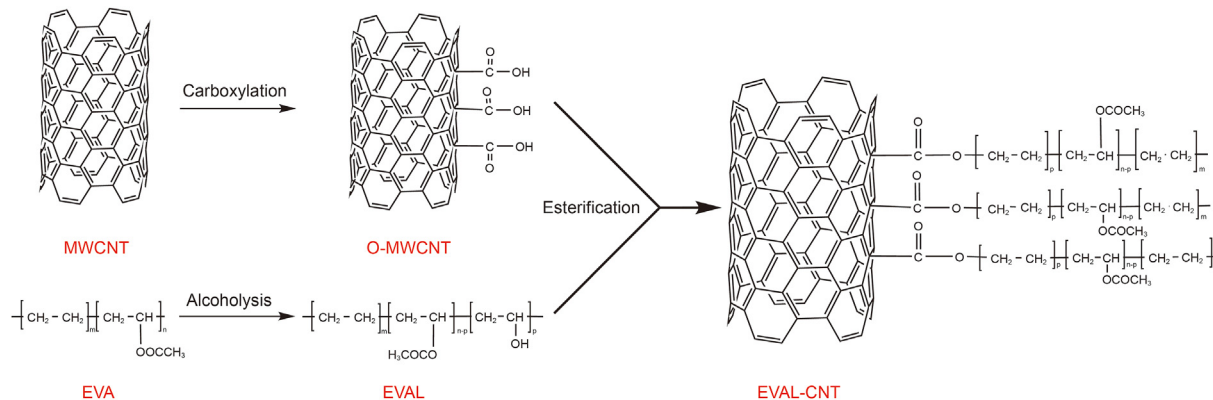


Fig. 2. Schematic diagram of the synthesis route of the novel nanocomposite EVAL-CNT.

### 3. Results and discussion

#### 3.1. Characterization of synthesized products

Fig. 3(a) shows the FTIR spectrum of EVAL, O-MWCNT and EVAL-CNT. In the FTIR spectrum of EVAL, the sharp peaks in 2905 and 1660  $\text{cm}^{-1}$  represent the stretching vibration of C–H and C=C, respectively. Moreover, peaks in the wavenumbers of 3445  $\text{cm}^{-1}$  assigned to the O–H bending vibrations provide evidence of the occurrence of alcoholysis reactions (Ren et al., 2017). Besides, in the FTIR spectrum of O-MWCNT, the peaks in 3548 and 1410  $\text{cm}^{-1}$  are related to the stretching vibration carboxyl groups (Elmesallamy et al., 2022). The peak around 1734 (C=O stretching vibration) and 1303  $\text{cm}^{-1}$  (single bond vibration of C–O–C) confirm the ester bond exists in the molecular structure of the EVAL-CNT nanocomposites, suggesting that chemical ester bonding has occurred between EVAL hydroxyl groups and O-MWCNT carboxyl group. It also could be seen that the main peaks of EVAL and O-MWCNT spectra are almost preserved in the EVAL-CNT spectrum. Overall, these results indicate that EVAL-CNT was successfully synthesized.

As shown in Fig. 3(b), there are two mass loss temperature regions for O-MWCNT, the first region is from 150 to 600  $^{\circ}\text{C}$ , and the mass loss in this temperature region is 29.86%, which is mainly caused by the removal of carboxyl groups (Datsyuk et al., 2008); The other mass loss zone is from 600 to 800  $^{\circ}\text{C}$ , and the mass loss in this zone is 6.92%, which is mainly caused by the decomposition of amorphous carbon and impurities left in the thermal oxidation process of O-MWCNT. In the EVAL-CNT curve, the mass loss before 300  $^{\circ}\text{C}$  is mainly due to the residual solvent, ash and moisture from the reaction during the grafting process, etc. The rapid mass loss after 300  $^{\circ}\text{C}$  is attributed to the slow decomposition of the polymer in the product. From Fig. 3(b), it can be obtained that the residual

masses of O-MWCNT and EVAL-CNT after pyrolysis were 64.23% and 2.16%, respectively. The grafting rate of EVAL-CNT was calculated as 62.07% based on the terminal weight loss rate.

The morphological characteristics of O-MWCNT and the product EVAL-CNT were observed using SEM, and the experimental results are shown in Fig. 3(d). It is apparent that O-MWCNT exhibits random distribution irregularly and tightly wound together due to its high specific surface area and surface activation energy. In comparison, the winding phenomenon of EVAL-CNT was significantly weaker and the tube diameter was thicker due to the grafting of organic material on its surface. The SEM image of the composite EVAL-CNT has some “white dots” compared to O-MWCNT, which are formed when the carbon nanotubes are pulled off and wrapped in the matrix by the polymer. The small amount of “white lines” is a small number of carbon nanotubes being pulled out and exposed in the form of white lines. It can be inferred that carbon nanotubes and EVAL have good interfacial bonding properties and the load can be transferred to carbon nanotubes effectively. Further, good homogeneous dispersion of the composite product in organic solvents was also observed from the dispersion photographs Fig. 3(c) of EVAL and EVAL-CNT in dodecane solution.

#### 3.2. Analysis of pour point reduction

The pour point reduction data of waxy crude oil after adding different mass fractions of PPDs are shown in Fig. 4. At the equivalent number of additives, the EVAL-CNT composite PPD showed superior reduction performance than EVA and EVAL. When EVA and EVAL were added separately, the pour point of the oil samples gradually decreased with the increase in dosage. In the case of EVAL-CNT, the overall trend of pour point drop gradually increases with the increase of the added amount, and then becomes stable or

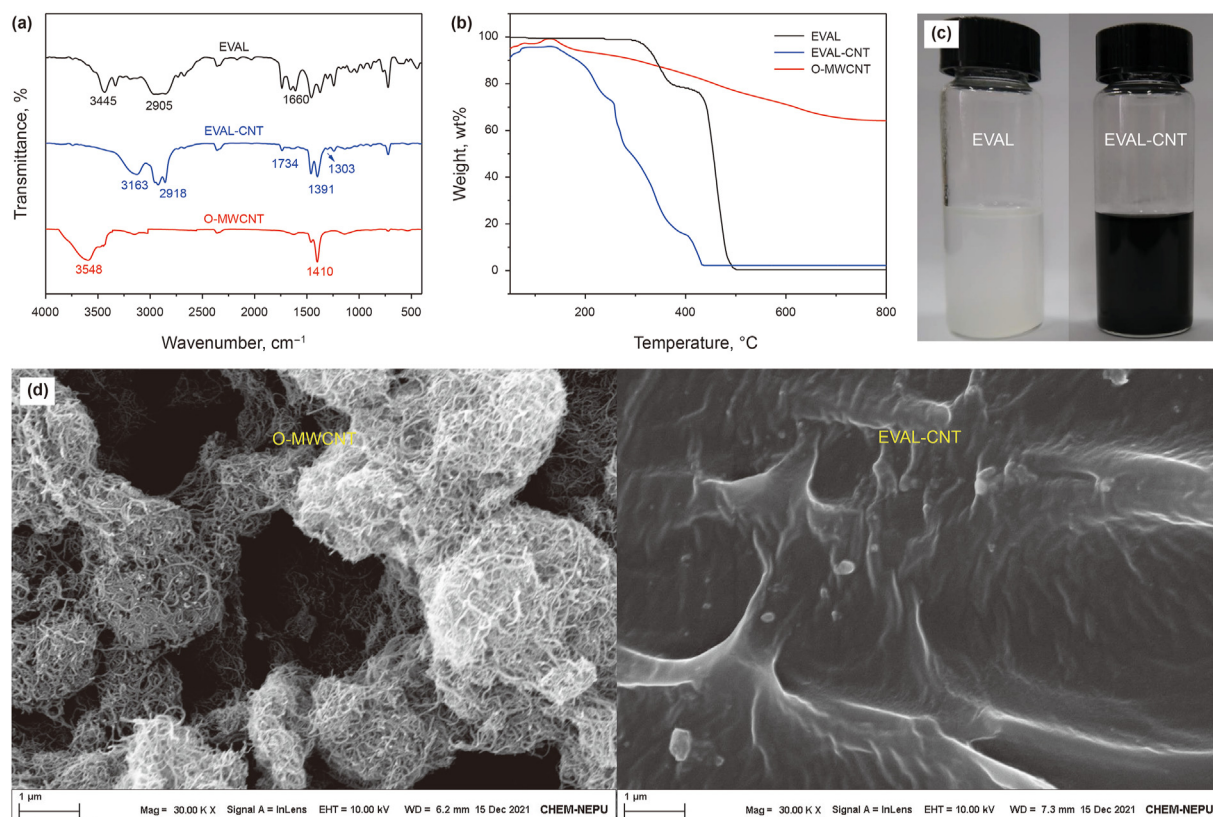


Fig. 3. Characterization of synthesized nanocomposites: (a) FTIR spectroscopy; (b) TGA curves; (c) dispersion status images; (d) scanning electron microscope images.

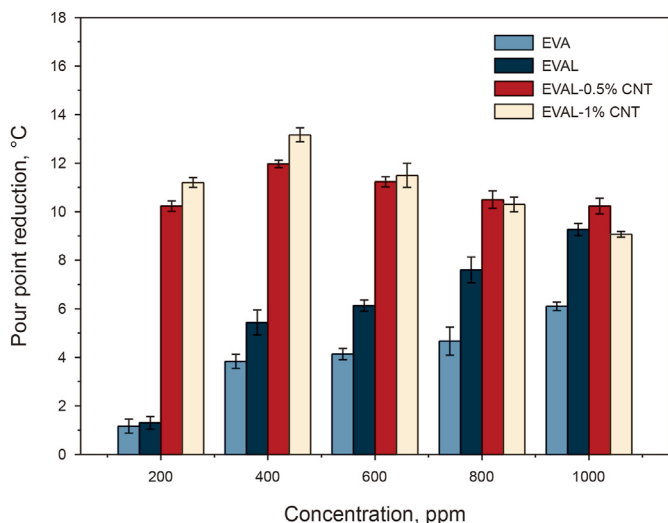


Fig. 4. Pour point drop of crude oil with different mass fractions of PPD.

decreases. When the mass fraction of EVAL-0.5% CNT was increased from 200 to 400, 600, 800 and 1000 ppm, the decrease of the freezing point was 10, 12, 11, 10 and 10 °C in order. For EVAL-1% CNT, the pour point decreases in the order of 11, 13, 12, 10 and 9 °C. When the mass fraction is 400 ppm, the pour point reduction effect is the best, and EVAL-1% CNT performs better than EVAL-0.5% CNT. A parallel comparison can also be made with the results of previous studies, where EVAL-GO at 1000 ppm resulted in a 12 °C drop in pour points (Liu et al., 2021), while EVAL-1% CNT resulted in a 13 °C drop in pour point at 400 ppm of addition.

### 3.3. Rheological properties

#### 3.3.1. Viscosity-temperature curve

Fig. 5 presents the experimental data on the apparent viscosity curves of crude oil with temperature before and after adding different mass fractions of EVAL-CNT at a constant shear rate of 20 s<sup>-1</sup> (Litvinets et al., 2016; Mun et al., 2022). During the high-temperature period, the additive dosage has almost no effect on the apparent viscosity, while it has a greater effect on the apparent viscosity in the low-temperature period. As the temperature

decreases, a large number of wax crystals in the oil precipitate out and form a spatial network structure, and the viscosity of the oil increases rapidly. At 15 °C, when 200, 400, 600, 800 and 1000 ppm EVAL-0.5% CNT was added, the apparent viscosity of wax oil was 29.6, 29.4, 31.2, 41.3 and 46.3 Pa·s in order, and the apparent viscosity of adding EVAL-1% CNT was 28.1, 23.9, 37.8, 48.2 and 63.4 Pa·s. The viscosity reduction efficiency is optimal at the dosage of 400 ppm.

The viscosity reduction results are consistent with their inhibitory effect on the pour point shown in Fig. 4. This can be explained by the fact that EVAL-CNT can act as a well-organized group to change the growth pattern of wax crystals, while the grafted ester group can effectively adsorb on the surface of wax crystals of waxy crude oil, further changing the growth tendency of wax crystals and thus reducing the viscosity of crude oil (Chen et al., 2020a). Besides, the inhibitory effect of EVAL-CNT is closely related to its dosage in the sample. The viscosity decreased and then increased with increasing dosage loading. An excessive amount of esterified polymer may produce a large number of crystals and interact with the formed crystals, which increases the viscosity of the sample and decreases the flow properties of the crude oil.

#### 3.3.2. Viscoelastic properties

Figs. 6 and 7 show the viscoelastic changes of the oil samples after adding different mass fractions of EVAL-0.5% CNT and EVAL-1% CNT, respectively. The viscoelastic curve could be divided into two parts: when the temperature is higher than the gelation point, the storage modulus ( $G'$ ) is smaller than the loss modulus ( $G''$ ), and the loss angle ( $\delta$ ) is greater than 45°, which means that the viscous response is dominant when the temperature is higher than the gelation point; however, when the temperature is lower than the gelation point, the storage modulus  $G'$  is larger than the loss modulus  $G''$ , and the loss angle  $\delta$  is less than 45°, which means that the elastic response is dominant. The gelation point is the conversion point of the oil sample from a sol to a gel (Yang et al., 2017).

As can be seen in Fig. 6(a), for the initial crude oil, the energy storage modulus and loss modulus are very small above 50 °C. As the temperature decreases,  $G'$  and  $G''$  grow significantly, indicating the beginning of a network precipitation aggregation and the formation of a gel structure with certain strength (Chen et al., 2020b; Deka et al., 2020). When the temperature is at 42.3 °C,  $G'$  and  $G''$  are equal, which means the gelation point of unadulterated waxy oil is 42.3 °C. When the temperature was below 35 °C,  $G'$  became large

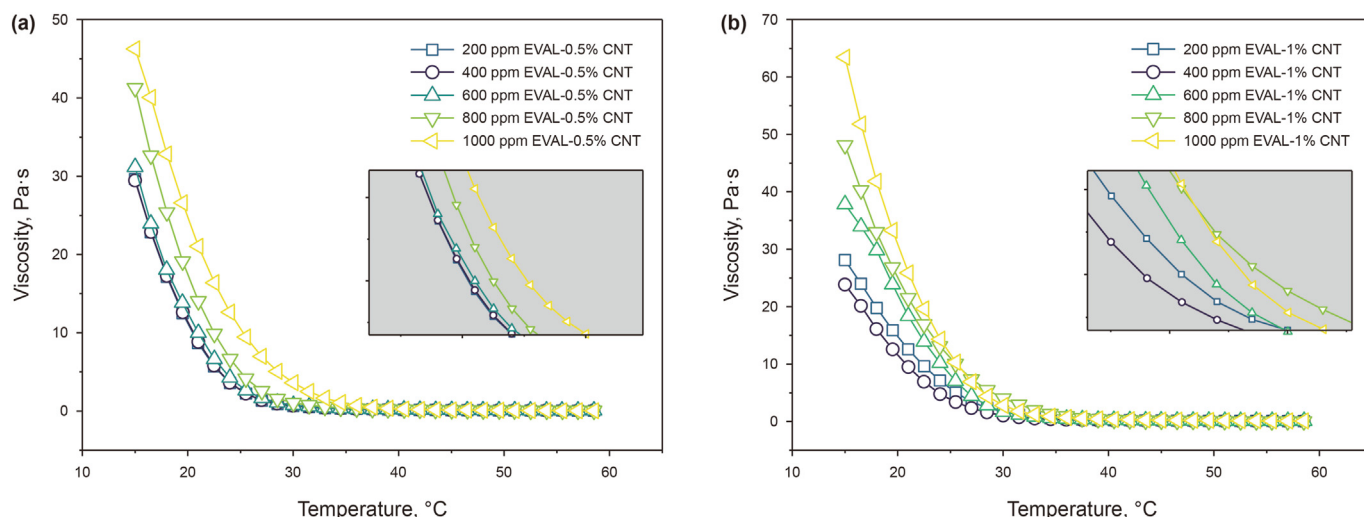
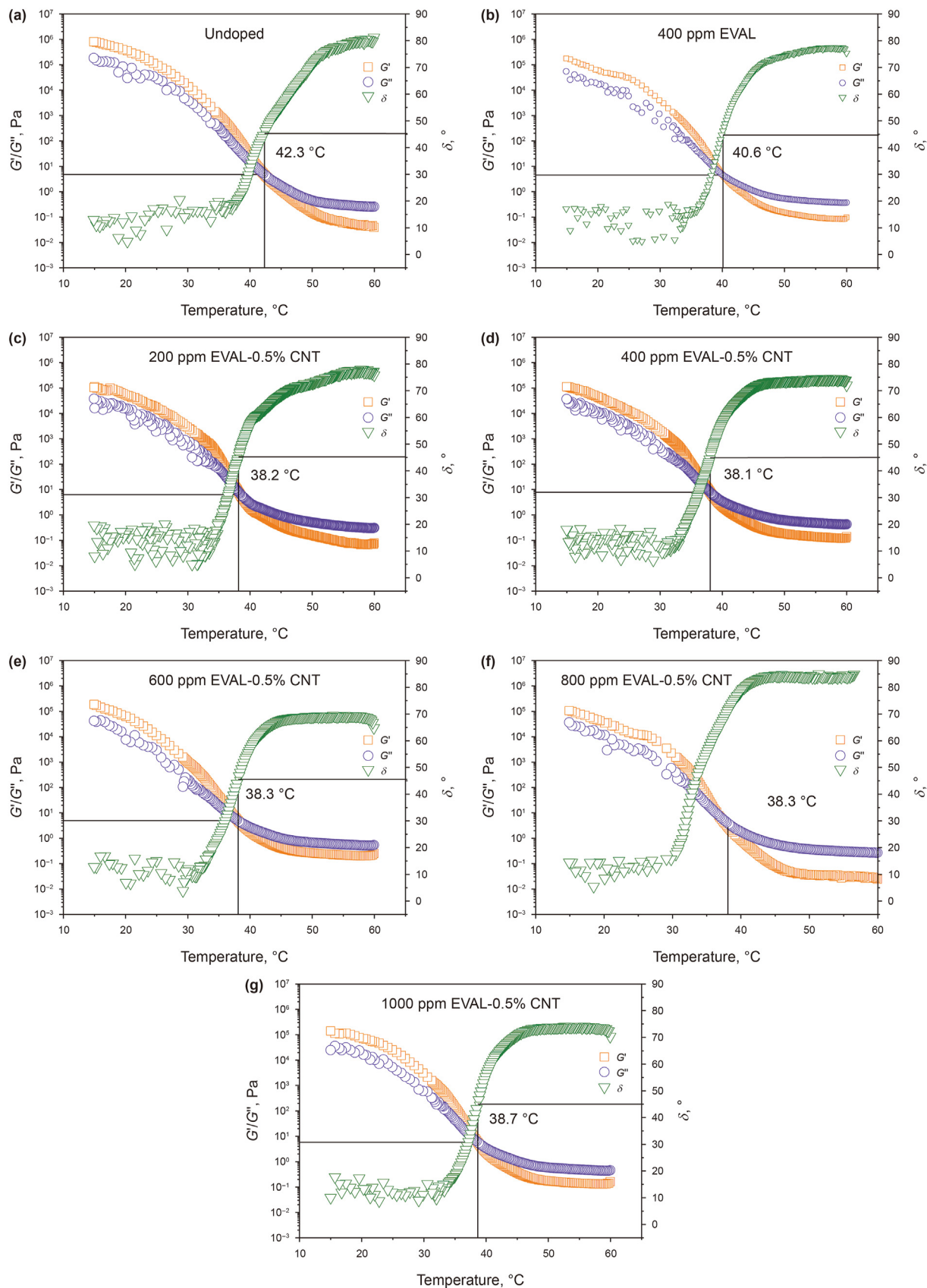


Fig. 5. The Viscosity-Temperature curves of treated oil samples doped with (a) EVAL-0.5% CNT, (b) EVAL-1% CNT.



**Fig. 6.** Viscoelasticity curves of the waxy crude oil doped with (a) undoped, (b) 400 ppm EVAL, (c) 200 ppm EVAL-0.5% CNT, (d) 400 ppm EVAL-0.5% CNT, (e) 600 ppm EVAL-0.5% CNT, (f) 800 ppm EVAL-0.5% CNT, (g) 1000 ppm EVAL-0.5% CNT.

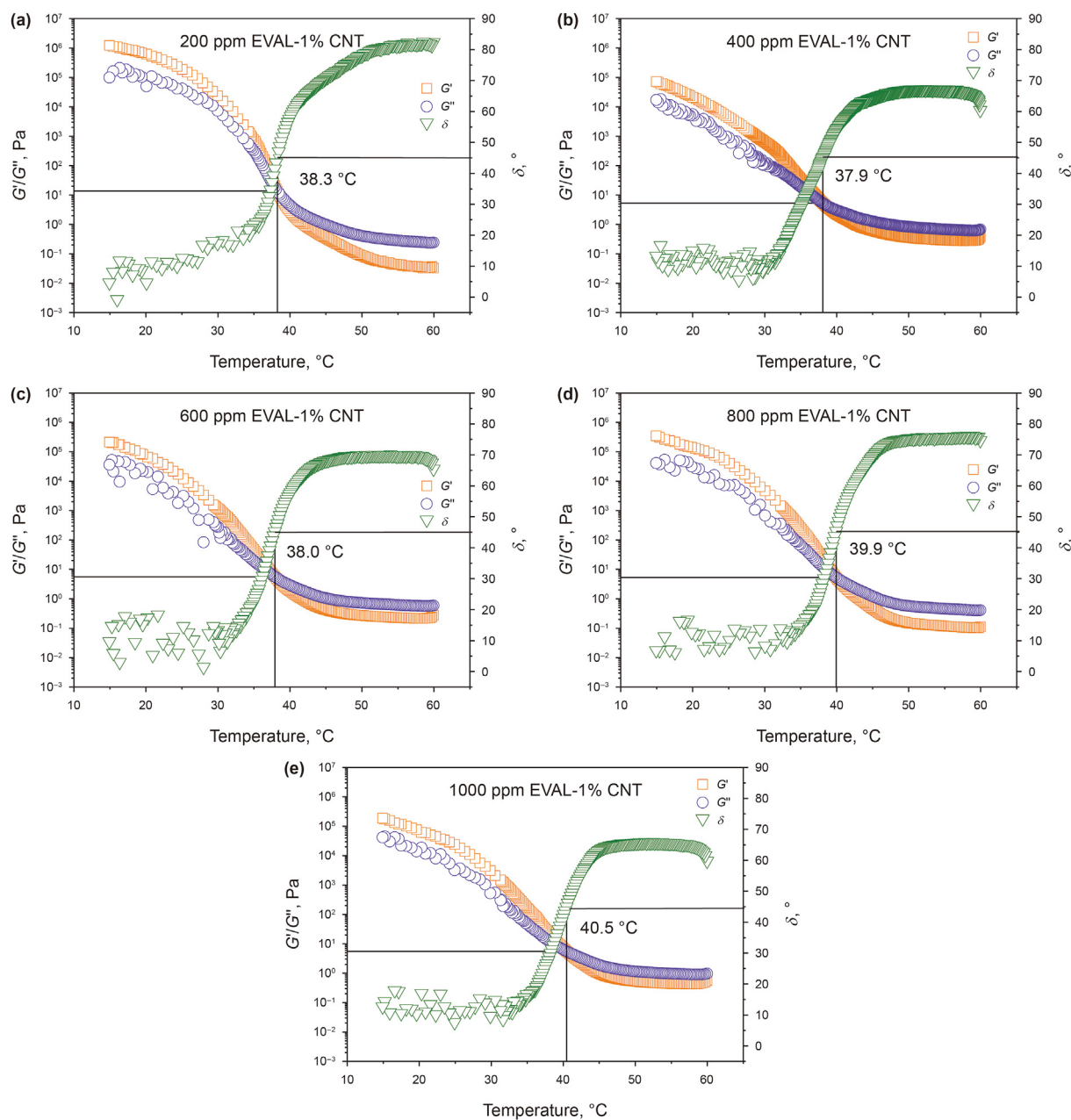


Fig. 7. Viscoelasticity curves of the waxy crude oil doped with different mass fractions of EVAL-1%CNT: (a) 200 ppm, (b) 400 ppm, (c) 600 ppm, (d) 800 ppm, (e) 1000 ppm.

and  $G'$  was higher than  $G''$ , which indicated that the wax oil changed to a more structural gel status at low temperatures. In Fig. 6(b), it can be obtained that the gel temperature of the oil sample decreased to 40.6 °C after the addition of 400 ppm EVAL. From Fig. 6(c)–(g) and Fig. 7(a)–(e), it is observed that when the mass fraction of the additive was 200, 400, 600, 800 and 1000 ppm, the gelation temperature of crude oil modified with EVAL-0.5% CNT was 38.2, 38.1, 38.3, 38.3 and 38.7 °C, and the gelation temperature of crude oil loaded with EVAL-1% CNT was 38.3, 37.9, 38.0, 39.9 and 40.5 °C in order.

As can be observed from Table 2 and Fig. 8, the gelation point of the unadulterated oil sample was 42.3 °C, and the  $G'$  and  $G''$  values at 15 °C were 801,242 and 185,085 Pa, respectively. The high  $G'$  and  $G''$  values indicated that the unadulterated oil sample had a very strong gelation structure at 15 °C. After the addition of 400 ppm EVAL, the gelation point of the oil was reduced to 40.6 °C, while the

Table 2

The  $G'$  and  $G''$  of the undoped/doped crude oil at 15 °C.

Crude oil sample	Dosage, ppm	$G'$ , Pa	$G''$ , Pa
Undoped	/	801,242	185,085
+EVA	400	400,581	90,841
+EVAL	400	177,597	54,759
+EVAL-0.5% CNT	400	113,076	36,788
+EVAL-1% CNT	400	72,048	17,036

$G'$  and  $G''$  values were significantly reduced to 177,597 and 54,759 Pa. The reduced  $G'$  and  $G''$  demonstrated that the strength of the gelling structure formed by the oil sample at 15 °C was significantly weakened by the addition of EVAL depressant. What stands out in the table is that after adding the same dosage of EVAL-1% CNT composite PPD, the gelation point,  $G'$  and  $G''$  of the oil

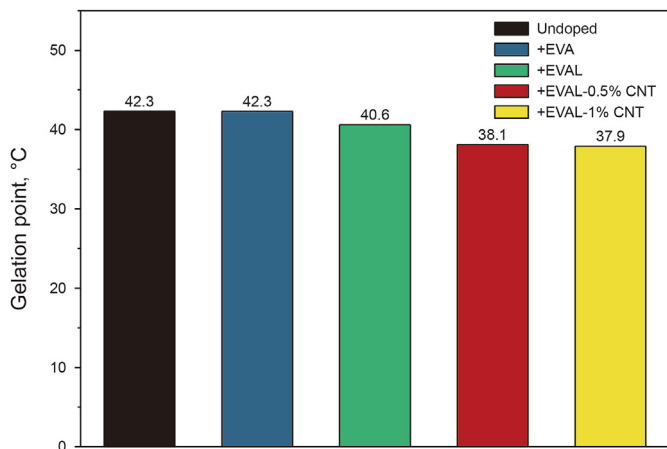


Fig. 8. Gelation point of waxy crude oil in different systems.

samples were further reduced, and the gelation point was further reduced by 2.7 °C compared with that of the EVAL-activated oil samples. Data from the study proved that the ability of the depressant to weaken the gelation structure of crude oil was further enhanced after the combination with carbon nanotubes.

### 3.3.3. Shear viscosity curve

In view of the results of the above analysis, the dynamic viscosity curve at the optimal dosage (400 ppm) was investigated experimentally. Fig. 9 illustrates the viscosity versus shear rate for crude oil blended with different types of PPD and virgin crude oil at 15, 25 and 35 °C (Al-Sabagh et al., 2016b; Yao et al., 2016). The apparent viscosities of the oil samples are higher at low shear rates, and with the increase of the shear rate, the apparent viscosities decrease significantly at first, but the decrease rate slows down after 100 s<sup>-1</sup> and finally stabilizes gradually. The viscosity of the initial crude oil is high and decreases when the oil sample is treated with PPD. In the comparison of the four groups of materials, EVAL-1%CNT showed excellent viscosity reduction performance at all test temperatures. There is a clear trend of decreasing viscosity in Fig. 8(a), which means that EVAL-1%CNT nanocomposite PPD exhibits excellent viscosity reduction performance at low temperatures.

The rheological behavior of crude oil added with PPD (400 ppm) at temperatures below or above the pour point (15, 25 and 35 °C) was compared with that of the unadulterated crude oil and the results are presented in Table 3. At a shear rate value of 79.78 s<sup>-1</sup>, the viscosity decreased by 85.4% for EVAL-1% CNT (from 17.61 to 2.57 Pa·s) and 58.7% for EVAL-0.5% CNT (from 17.61 to 7.27 Pa·s) at 15 °C, while the viscosity decreased by 44.9% with virgin EVA (from 17.61 to 9.71 Pa·s). In addition, it can be concluded in the table that the viscosity decreases with increasing temperature due to the dissolution of wax crystals in the crude oil. The reduction in sample viscosity was attributed to the para-wax crystal effect of the nanocomposite, where the carbon nanotubes effectively reduced the formation of a three-dimensional network of wax crystals, allowing only a limited number of wax crystals to network, ensuring easier mobility of the oil sample at low temperatures. Thus, the experimental data also indicated the significant effectiveness of EVAL-CNT in viscosity reduction as well.

### 3.3.4. Yield characteristics

The yield curves of the initial crude oil and the crude oil loaded with different types of PPD at a temperature of 15 °C are shown in Fig. 10(a), and the corresponding yield values are shown in

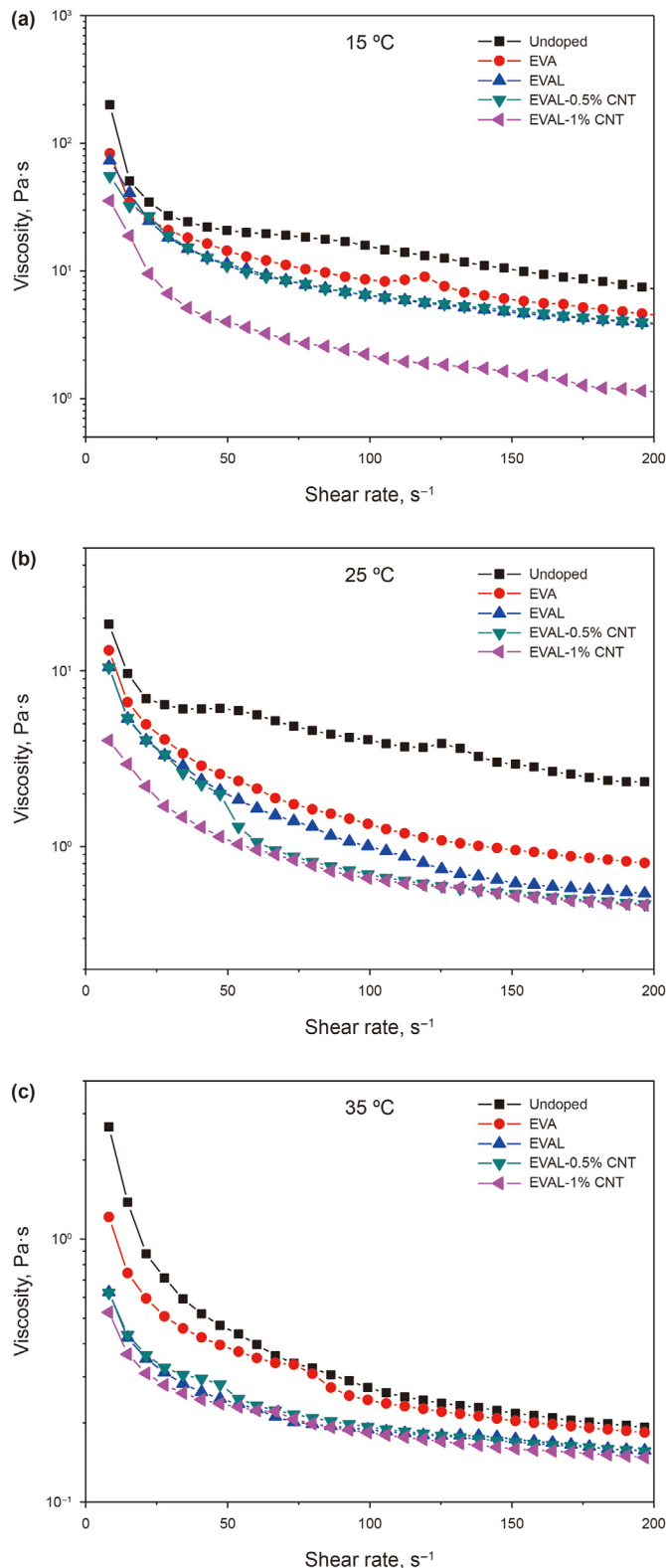


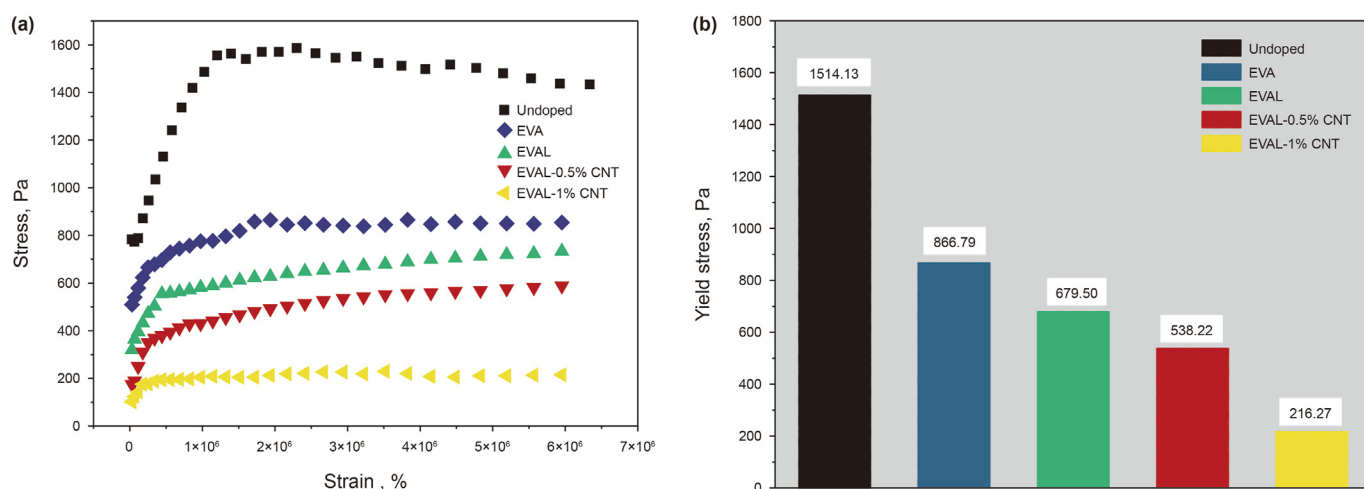
Fig. 9. Relation between shear rate and viscosity for undoped and doped crude oil at different temperatures: (a) 15 °C, (b) 25 °C, (c) 35 °C.

Fig. 10(b). The yield value of the oil sample with the addition of 400 ppm EVAL depressant was 679.5 Pa, which was 55.1% lower compared to the virgin crude oil (1514.13 Pa), and 64.5% lower for the same concentration of EVAL-0.5%CNT. The best-performing



**Table 3**  
Effects of different PPDs on the transient apparent viscosity of waxy crude oil.

Oil Sample	Temperature, °C	Viscosity, Pa·s			
		21.30 s <sup>-1</sup>	79.78 s <sup>-1</sup>	138.30 s <sup>-1</sup>	196.77 s <sup>-1</sup>
Undoped	15	34.61	17.61	11.00	7.08
	25	6.96	4.57	3.25	2.37
	35	0.87	0.32	0.23	0.19
+EVA	15	26.93	9.71	6.41	5.14
	25	4.95	1.63	1.00	0.81
	35	0.59	0.30	0.21	0.18
+EVAL	15	25.37	7.30	5.14	3.85
	25	4.01	1.29	0.68	0.54
	35	0.36	0.20	0.18	0.16
+EVAL-0.5% CNT	15	24.62	7.27	4.97	3.80
	25	4.03	0.82	0.56	0.47
	35	0.35	0.19	0.17	0.16
+EVAL-1% CNT	15	9.50	2.57	1.73	1.12
	25	2.20	0.78	0.56	0.46
	35	0.30	0.19	0.16	0.15



**Fig. 10.** Comparison of yield properties of initial crude oil and doped crude oil.

EVAL-1%CNT nanocomposite reduced the yield value to 216.27 Pa, a reduction of 85.7% from the initial oil sample. The result shows that the gelling structure formed by the crude oil with EVAL-CNT is inferior to that with conventional PPD, which is easy to be destroyed. The reduction of yield value can reduce the peak pressure of crude oil pipeline shutdown and restart, and improve the safety of pipeline operation, which has practical engineering significance.

### 3.4. Microstructural properties of wax crystals

The effects of EVAL-CNT composite PPD on the microstructural properties of wax crystals from Daqing crude oil are shown in Fig. 11. For virgin crude oil the wax crystals precipitated were large in number and small in size, showing a messy ordering in the oil phase system. Fig. 11(b)–(f) demonstrate the wax crystal morphology of wax oils with different mass fractions of EVAL-CNT additions at 15 °C. The graph reveals that the distribution of wax crystals in the oil before the addition of the PPD is large and the profile is small. With the addition of the EVAL-CNT, the wax crystals show a striped distribution, and the distribution range is reduced, the outline is clear, and the space not occupied by wax crystals is obviously increased. Changes in the microscopic morphology of the wax crystals can reflect some extent the degree of improvement in

the macroscopic rheology of the crude oil by the depressant. At lower dosing rates, the wax content within the crude oil system is relatively high and the effective concentration of PPD is low, which will result in a low inhibition effect as PPD cannot fully interact with the wax crystals. Moreover, due to the large specific surface area of MWCNTs and the strong van der Waals attraction between carbon tubes, excessive amounts of MWCNTs are very prone to agglomeration in the polymer matrix and cannot take full advantage of their structure and properties. Therefore, the inhibition of wax crystals decreases with increasing additions. And the increase in the crystallization ability of waxes leads to an increase in the pour point of crude oil containing waxes, which explains the phenomenon that the pour point first decreases and then increases.

### 3.5. Mechanism

From the above experimental results and the microscopic image analysis of the wax crystals, it can be deduced that EVAL-CNT nanocomposite PPD provides a “heterogeneous crystallization template” for the precipitation of wax crystals during the cooling down process of wax molecule crystallization, which promotes the precipitation of wax molecules and makes the wax crystals show a striped distribution with clear outlines. The schematic diagram of the mechanism is shown in Fig. 12. This is also consistent with

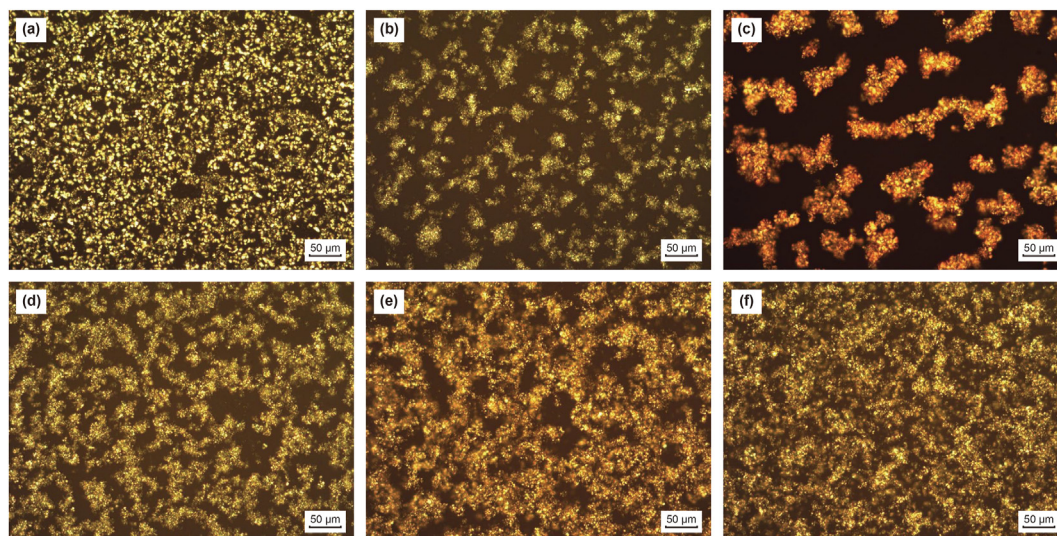


**Fig. 11.** Polarized microscopic images of crude oil doped with different dosages of EVAL-1%CNT at 15 °C: (a) 0; (b) 200 ppm; (c) 400 ppm; (d) 600 ppm; (e) 800 ppm; (f) 1000 ppm.

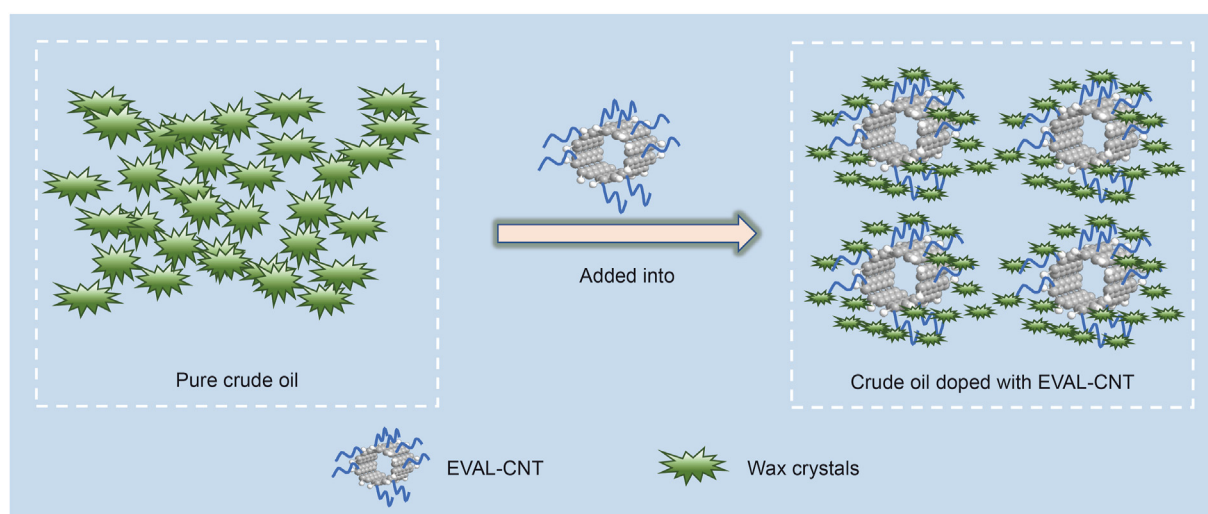


**Fig. 12.** Schematic diagram of performance improving mechanism of the nanocomposite PPD on wax crystals.

classical nucleation theory, as nanocomposites are heterogeneous nucleation systems with many “EVAL-CNT” two-phase interfaces between the carbon tubes and the EVAL matrix, where the Gibbs free energy required for nucleation is relatively low, making nucleation easier. The tubular structure of carbon nanotubes also makes the microscopic pictures of wax crystals show a different morphology from that of EVAL-GO.

Carbon nanotubes provide nucleation sites for the heterogeneous nucleation process, thus further narrowing the crystal-liquid interface, contributing to the formation of a more compact wax crystal structure and inhibiting the formation of network-like wax crystals. These led to the reduction of crude oil viscosity, improved low-temperature flow properties, and weakened the gel structure formed in crude oil at low temperatures. Adequate amounts of MWCNT can be dispersed uniformly in the shallow layers of the EVAL surface, providing nucleation sites for heterogeneous nucleation in these regions, and at the same time the carbon tubes are isolated from each other and do not interfere with each other, so the addition of adequate amounts of carbon nanotubes is beneficial for activity enhancement. However, when the addition level is

excessive (>400 ppm), the carbon nanotubes and their agglomerates stack on top of each other, connect and form a continuous network structure. In this case, the further increase in the content of carbon tubes is of limited use in “promoting heterogeneous nucleation” and the strong interaction between the carbon tubes and their agglomerates leads to irregular precipitation of wax crystals, which deteriorates the flow properties of the crude oil.

#### 4. Conclusions

Based on previous studies, carbon nanotube materials were introduced into the crude oil fluidity study system through chemical grafting, and the effects of the additional amount on the pour point and rheological properties of Daqing crude oil were highlighted. EVAL-CNT reduced the pour point of wax oil by 13 °C and the low-temperature viscosity by 85.4% at the same dosage rate and treatment temperature, further inhibiting the formation of the three-dimensional network structure of wax crystals and further weakening the structural strength and viscoelasticity of the modified gelling oil. The research results in this paper have some

reference value for the application of polymer-based carbon nanotube composites in the field of crude oil transportation.

### Declaration of competing interest

The authors declare that they have no known competing financial interests or personal relationships that could have appeared to influence the work reported in this paper.

### References

- Aiyejina, A., Chakrabarti, D.P., Pilgrim, A., et al., 2011. Wax formation in oil pipelines: a critical review. *Int. J. Multiphas. Flow* 37 (7), 671–694. <https://doi.org/10.1016/j.jmultiphaseflow.2011.02.007>.
- Al-Sabagh, A.M., Betiha, M.A., Osman, D.I., et al., 2016a. A new covalent strategy for functionalized montmorillonite-poly(methyl methacrylate) for improving the flowability of crude oil. *RSC Adv.* 6 (111), 109460–109472. <https://doi.org/10.1039/c6ra21319g>.
- Al-Sabagh, A.M., Betiha, M.A., Osman, D.I., et al., 2016b. Preparation and evaluation of poly (methyl methacrylate)-graphene oxide nanohybrid polymers as pour point depressants and flow improvers for waxy crude oil. *Energy Fuel*. 30 (9), 7610–7621. <https://doi.org/10.1021/acs.energyfuels.6b01105>.
- Alemi, F.M., Dehghani, S.A.M., Rashidi, A., et al., 2021a. A mechanistic study toward the effect of single-walled carbon nanotubes on asphaltene precipitation and aggregation in unstable crude oil. *J. Mol. Liq.* 330, 115594. <https://doi.org/10.1016/j.molliq.2021.115594>.
- Alemi, F.M., Dehghani, S.A.M., Rashidi, A., et al., 2021b. Synthesis of MWCNT-Fe<sub>2</sub>O<sub>3</sub> nanocomposite for controlling formation and growth of asphaltene particles in unstable crude oil. *Colloid. Surface.* 615, 126295. <https://doi.org/10.1016/j.colsurfa.2021.126295>.
- Alves, B.F., Rossi, T.M., Marques, L.C.C., et al., 2023. Composites of EVA and hydrophobically modified PAMAM dendrimer: effect of composition on crystallization and flow assurance of waxy systems. *Fuel* 332, 125962. <https://doi.org/10.1016/j.fuel.2022.125962>.
- Chen, F.F., Liu, J.B., Yang, T.S., et al., 2020a. Influence of maleic anhydride-co-methyl benzyl acrylate copolymers modified with long-chain fatty amine and long-chain fatty alcohol on the cold flow properties of diesel fuel. *Fuel* 268, 117392. <https://doi.org/10.1016/j.fuel.2020.117392>.
- Chen, J., Rao, A.M., Lyuksyutov, S., et al., 2001. Dissolution of full-length single-walled carbon nanotubes. *J. Phys. Chem. B* 105 (13), 2525–2528. <https://doi.org/10.1021/jp002596i>.
- Chen, X.Y., Li, C.X., Liu, D.W., et al., 2020b. Effect of doped emulsifiers on the morphology of precipitated wax crystals and the gel structure of water-in-model-oil emulsions. *Colloid. Surface.* 607, 125434. <https://doi.org/10.1016/j.colsurfa.2020.125434>.
- Chen, C.H., Zhang, J.J., Ma, C.B., et al., 2019. Influence of wax precipitation on the impedance spectroscopy of waxy oils. *Energy Fuels* 33 (10), 9767–9778. <https://doi.org/10.1021/acs.energyfuels.9b02543>.
- Chi, Y.D., Yang, J.H., Sarica, C., et al., 2019. A critical review of controlling paraffin deposition in production lines using chemicals. *Energy Fuels* 33 (4), 2797–2809. <https://doi.org/10.1021/acs.energyfuels.9b00316>.
- Colunga, J.G.M., Sanchez-Valdes, S., de Valle, L.F.R., et al., 2021. Anhydride grafting on carbon nanotubes using ultrasound and its effect on polypropylene nanocomposite properties. *Polym-Plast. Tech. Mat.* 60 (10), 1066–1083. <https://doi.org/10.1080/25740881.2021.1876881>.
- Datsyuk, V., Kalyva, M., Papagelis, K., et al., 2008. Chemical oxidation of multiwalled carbon nanotubes. *Carbon* 46 (6), 833–840. <https://doi.org/10.1016/j.carbon.2008.02.012>.
- Deka, B., Sharma, R., Mahto, V., 2020. Synthesis and performance evaluation of poly (fatty esters-co-succinic anhydride) as pour point depressants for waxy crude oils. *J. Petrol. Sci. Eng.* 191, 107153. <https://doi.org/10.1016/j.petrol.2020.107153>.
- Ding, J.H., Rahman, O.U., Peng, W.J., et al., 2018. A novel hydroxyl epoxy phosphate monomer enhancing the anticorrosive performance of waterborne Graphene/Epoxy coatings. *Appl. Surf. Sci.* 427, 981–991. <https://doi.org/10.1016/j.apsusc.2017.08.224>.
- Elmesallamy, S.M., Fekry, M., Hussein, L.I., et al., 2022. Polybenzoxazine/carbon nanotube nanocomposites as a polymeric sensing material for volatile organic compounds. *J. Polym. Res.* 29 (8), 338. <https://doi.org/10.1007/s10965-022-03169-1>.
- He, C.Z., Ding, Y.F., Chen, J., et al., 2016. Influence of the nano-hybrid pour point depressant on flow properties of waxy crude oil. *Fuel* 167, 40–48. <https://doi.org/10.1016/j.fuel.2015.11.031>.
- Huang, H.R., Wang, W., Peng, Z.H., et al., 2020a. Synergistic effect of magnetic field and nanocomposite pour point depressant on the yield stress of waxy model oil. *Petrol. Sci.* 17 (3), 838–848. <https://doi.org/10.1007/s12182-019-00418-9>.
- Huang, H.R., Wang, W., Peng, Z.H., et al., 2020b. Magnetic organic-inorganic nanohybrid for efficient modification of paraffin hydrocarbon crystallization in model oil. *Langmuir* 36 (2), 591–599. <https://doi.org/10.1021/acs.langmuir.9b03278>.
- Jaberi, I., Khosravi, A., Rasouli, S., 2020. Graphene oxide-PEG: an effective anti-wax precipitation nano-agent in crude oil transportation. *Upstream Oil Gas Technol.* 5, 100017. <https://doi.org/10.1016/j.upstre.2020.100017>.
- Kashefi, M.H., Saedodin, S., Rostamian, S.H., 2021. Effect of silica nano-additive on flash point, pour point, rheological and tribological properties of lubricating engine oil: an experimental study. *J. Therm. Anal. Calorim.* 147, 4073–4086. <https://doi.org/10.1007/s10973-021-10812-4>.
- Lei, Y., Han, S.P., Zhang, J.J., 2016. Effect of the dispersion degree of asphaltene on wax deposition in crude oil under static conditions. *Fuel Process. Technol.* 146, 20–28. <https://doi.org/10.1016/j.fuproc.2016.02.005>.
- Li, Y.J., Li, C.X., Sun, G.Y., et al., 2020. Characterization of the precipitation modes of paraffin wax in water-in-model-oil emulsions. *Energy Fuels* 34 (12), 16014–16022. <https://doi.org/10.1021/acs.energyfuels.0c02902>.
- Liang, T., Hou, J.R., Qu, M., et al., 2022. Application of nanomaterial for enhanced oil recovery. *Petrol. Sci.* 19 (2), 882–899. <https://doi.org/10.1016/j.petsci.2021.11.011>.
- Lin, Y., Xu, K., Cao, X., et al., 2021. Role of nanotube chirality on the mechanical characteristics of pillared graphene. *Mech. Mater.* 162, 104035. <https://doi.org/10.1016/j.mechmat.2021.104035>.
- Lin, Y., Zhou, B., Fernando, K.A.S., et al., 2003. Polymeric carbon nanocomposites from carbon nanotubes functionalized with matrix polymer. *Macromolecules* 36 (19), 7199–7204. <https://doi.org/10.1021/ma0348876>.
- Litvinets, I.V., Prozorova, I.V., Yudina, N.V., et al., 2016. Effect of ammonium-containing polyalkyl acrylate on the rheological properties of crude oils with different ratio of resins and waxes. *J. Petrol. Sci. Eng.* 146, 96–102. <https://doi.org/10.1016/j.petrol.2016.04.026>.
- Liu, Y., Sun, Z.N., Jing, G.L., et al., 2021. Synthesis of chemical grafting pour point depressant EVAL-GO and its effect on the rheological properties of Daqing crude oil. *Fuel Process. Technol.* 223, 107000. <https://doi.org/10.1016/j.fuproc.2021.107000>.
- Ma, W.J., Jiang, Z.C., Lu, T., et al., 2022. Lightweight, elastic and superhydrophobic multifunctional nanofibrous aerogel for self-cleaning, oil/water separation and pressure sensing. *Chem. Eng. J.* 430, 132989. <https://doi.org/10.1016/j.cej.2021.132989>.
- Mahmoud, T., Betiha, M.A., 2021. Poly(octadecyl acrylate-co-vinyl neodecanoate)/oleic acid-modified nano-graphene oxide as a pour point depressant and an enhancer of waxy oil transportation. *Energy Fuels* 35 (7), 6101–6112. <https://doi.org/10.1021/acs.energyfuels.1c00034>.
- Martinez-Palou, R., Mosqueira, M.D., Zapata-Rendon, B., et al., 2011. Transportation of heavy and extra-heavy crude oil by pipeline: a review. *J. Petrol. Sci. Eng.* 75 (3–4), 274–282. <https://doi.org/10.1016/j.petrol.2010.11.020>.
- Moud, A.A., 2022. Asphaltene induced changes in rheological properties: a review. *Fuel* 316, 123372. <https://doi.org/10.1016/j.fuel.2022.123372>.
- Mu, S., Liu, K., Li, H., et al., 2022. Microwave-assisted synthesis of highly dispersed ZrO<sub>2</sub> on CNTs as an efficient catalyst for producing 5-hydroxymethylfurfural (5-HMF). *Fuel Process. Technol.* 233, 107292. <https://doi.org/10.1016/j.fuproc.2022.107292>.
- Mun, G.A., Bekbassov, T., Bek Sultanov, Z., et al., 2022. Modified graft copolymers based on ethylene vinyl acetate as depressants for waxy crude oil and their effect on the rheological properties of oil. *J. Petrol. Sci. Eng.* 213, 110298. <https://doi.org/10.1016/j.petrol.2022.110298>.
- Oliveira, L.M.S.L., Nunes, R.C.P., Melo, I.C., et al., 2016. Evaluation of the correlation between wax type and structure/behavior of the pour point depressant. *Fuel Process. Technol.* 149, 268–274. <https://doi.org/10.1016/j.fuproc.2016.04.024>.
- Qu, M., Liang, T., Hou, J., et al., 2022. Laboratory study and field application of amphiphilic molybdenum disulfide nanosheets for enhanced oil recovery. *J. Petrol. Sci. Eng.* 208, 109695. <https://doi.org/10.1016/j.petrol.2021.109695>.
- Ren, Y.W., Chen, Z.J., Du, H., et al., 2017. Preparation and evaluation of modified ethylene vinyl acetate copolymer as pour point depressant and flow improver for Jiangnan crude oil. *Ind. Eng. Chem. Res.* 56 (39), 11161–11166. <https://doi.org/10.1021/acs.iecr.7b02929>.
- Sepelhrnia, M., Mohammadzadeh, K., Veyseh, M.M., et al., 2022. Rheological behavior of engine oil based hybrid nanofluid containing MWCNTs and ZnO nanopowders: experimental analysis, developing a novel correlation, and neural network modeling. *Powder Technol.* 404, 117492. <https://doi.org/10.1016/j.powtec.2022.117492>.
- Sharma, R., Deka, B., Mahto, V., et al., 2019. Investigation into the flow assurance of waxy crude oil by application of graphene-based novel nanocomposite pour point depressants. *Energy Fuels* 33 (12), 12330–12345. <https://doi.org/10.1021/acs.energyfuels.9b03124>.
- Sharma, R., Deka, B., Mahto, V., et al., 2022. Experimental investigation into the development and evaluation of ionic liquid and its graphene oxide nanocomposite as novel pour point depressants for waxy crude oil. *J. Petrol. Sci. Eng.* 208, 109691. <https://doi.org/10.1016/j.petrol.2021.109691>.
- Singh, N.K., Singh, Y., Sharma, A., et al., 2021. Rheological characteristics and tribological performance of neem biodiesel-based nano oil added with MWCNT. *Biomass Convers. Biorefinery.* <https://doi.org/10.1007/s13399-021-01919-7>.
- Soni, H.P., Kiranbala, Agrawal, K.S., et al., 2010. Designing maleic anhydride-alpha-olfin copolymeric combs as wax crystal growth nucleators. *Fuel Process. Technol.* 91 (9), 997–1004. <https://doi.org/10.1016/j.fuproc.2010.02.019>.
- Subramanie, P., Vijayakumar, S.D., Ridzuan, N., 2021. Effect of wax inhibitor and sodium chloride, Na<sup>+</sup> nanoparticle on wax deposition of Malaysian crude oil through cold finger analysis. *Petrol. Sci. Technol.* 39 (19–20), 860–877. <https://doi.org/10.1080/10916466.2021.1973496>.
- Wang, C., Chen, H., Shi, H., et al., 2022. Role of a nanocomposite pour point depressant on wax deposition in different flow patterns from the perspective of crystallization kinetics. *ACS Omega* 7 (13), 11200–11207. <https://doi.org/10.1021/acscentsci.2c00000>.

- 10.1021/acsomega.2c00068.
- Wang, C.S., Zhang, M., Wang, W., et al., 2020. Experimental study of the effects of a nanocomposite pour point depressant on wax deposition. *Energy Fuels* 34 (10), 12239–12246. <https://doi.org/10.1021/acs.energyfuels.0c02001>.
- Wu, J., He, J., Odegard, G.M., et al., 2013a. Giant stretchability and reversibility of tightly wound helical carbon nanotubes. *J. Am. Chem. Soc.* 135 (37), 13775–13785. <https://doi.org/10.1021/ja404330q>.
- Wu, J., Nagao, S., He, J., et al., 2013b. Nanohinge-induced plasticity of helical carbon nanotubes. *Small* 9 (21), 3561–3566. <https://doi.org/10.1002/sml.201202830>.
- Wu, J., Shi, Q., Zhang, Z., et al., 2018a. Nature-inspired entwined coiled carbon mechanical metamaterials: molecular dynamics simulations. *Nanoscale* 10 (33), 15641–15653. <https://doi.org/10.1039/C8NR04507K>.
- Wu, J., Zhao, H., Liu, J., et al., 2018b. Nanotube-chirality-controlled tensile characteristics in coiled carbon metastructures. *Carbon* 133, 335–349. <https://doi.org/10.1016/j.carbon.2018.03.055>.
- Xia, X., Li, C.X., Sun, G.Y., et al., 2022a. Performance improvement of ethylene–vinyl acetate copolymer pour point depressant (EVA PPD) by adding small dosages of laurylamine (LA). *Petrol. Sci.* 19 (5), 2472–2482. <https://doi.org/10.1016/j.petsci.2022.04.002>.
- Xia, X., Li, C., Dai, S., et al., 2022b. Modification effect of macroporous comb-like polymeric pour point depressants on the flow behavior of model waxy oils. *Fuel* 314, 123113. <https://doi.org/10.1016/j.fuel.2021.123113>.
- Xu, J., Xing, S.L., Qian, H.Q., et al., 2013. Effect of polar/nonpolar groups in comb-type copolymers on cold flowability and paraffin crystallization of waxy oils. *Fuel* 103, 600–605. <https://doi.org/10.1016/j.fuel.2012.06.027>.
- Yang, F., Yao, B., Li, C.X., et al., 2017. Performance improvement of the ethylene-vinyl acetate copolymer (EVA) pour point depressant by small dosages of the poly-methylsilsesquioxane (PMSQ) microsphere: an experimental study. *Fuel* 207, 204–213. <https://doi.org/10.1016/j.fuel.2017.06.083>.
- Yang, F., Zhang, X.P., Li, C.X., et al., 2019a. Poly(aminopropyl/methyl)silsesquioxane microspheres improve the flowability of model waxy oils associated with asphaltenes. *Fuel* 243, 60–69. <https://doi.org/10.1016/j.fuel.2019.01.116>.
- Yang, S., Li, C.X., Yang, F., et al., 2019b. Effect of polyethylene-vinyl acetate pour point depressants on the flow behavior of degassed Changqing waxy crude oil before/after scCO<sub>2</sub> extraction. *Energy Fuels* 33 (6), 4931–4938. <https://doi.org/10.1021/acs.energyfuels.9b00561>.
- Yao, B., Li, C.X., Yang, F., et al., 2016. Organically modified nano-clay facilitates pour point depressing activity of polyoctadecylacrylate. *Fuel* 166, 96–105. <https://doi.org/10.1016/j.fuel.2015.10.114>.
- Yao, B., Li, C.X., Yang, F., et al., 2018. Ethylene-vinyl acetate copolymer and resin-stabilized asphaltenes synergistically improve the flow behavior of model waxy oils. 1. Effect of wax content and the synergistic mechanism. *Energy Fuels* 32 (2), 1567–1578. <https://doi.org/10.1021/acs.energyfuels.7b03657>.
- Zhang, X., Li, N., Wei, Z., et al., 2022. Synthesis of nano-hybrid polymethacrylate-carbon dots as pour point depressant and combined with ethylene-vinyl acetate resin to improve the cold flow properties of diesel fuels. *Energy* 253, 124186. <https://doi.org/10.1016/j.energy.2022.124186>.
- Zhao, Z.C., Yan, S., Lian, J., et al., 2018. A new kind of nanohybrid poly(tetradecyl methyl-acrylate)-graphene oxide as pour point depressant to evaluate the cold flow properties and exhaust gas emissions of diesel fuels. *Fuel* 216, 818–825. <https://doi.org/10.1016/j.fuel.2017.07.087>.